Identification of a chronic non-neurodegenerative microglia activation state in a mouse model of peroxisomal β-oxidation deficiency

(Article begins on next page)

07 January 2023

Identification of a chronic non-neurodegenerative microglia activation state in a mouse model of peroxisomal β-oxidation deficiency

Simon Verheijden[1,*], **Lien Beckers**[1,*], **Andrea Casazza**[2,3], **Oleg Butovsky**[4], **Massimiliano Mazzone**[2,3], and **Myriam Baes**[1]

[1]KU Leuven - University of Leuven, Department of Pharmaceutical and Pharmacological Sciences, Cell Metabolism, B-3000 Leuven, Belgium

[2]KU Leuven - University of Leuven, Department of Oncology, Laboratory of Molecular Oncology and Angiogenesis, B-3000 Leuven, Belgium

[3]VIB, Vesalius Research Center, Laboratory of Molecular Oncology and Angiogenesis, B-3000 Leuven, Belgium

[4]Center for Neurologic Diseases, Department of Neurology, Brigham and Women's Hospital, Harvard Medical School, Boston, Massachusetts, USA

Abstract

The functional diversity and molecular adaptations of reactive microglia in the chronically inflamed central nervous system (CNS) are poorly understood. We previously showed that mice lacking multifunctional protein 2 (MFP2), a pivotal enzyme in peroxisomal β-oxidation, persistently accumulate reactive myeloid cells in the gray matter of the CNS. Here we show that the increased numbers of myeloid cells solely derive from proliferation of resident microglia and not from infiltrating monocytes. We defined the signature of $Mfp2^{-/-}$ microglia by gene expression profiling after acute isolation, which was validated by quantitative PCR, immunohistochemical and flow cytometric analysis. The features of $Mfp2^{-/-}$ microglia were compared with those from SOD1^{G93A} mice, an amyotrophic lateral sclerosis model. In contrast to the neurodegenerative milieu of SOD1^{G93A} spinal cord, neurons were intact in $Mfp2^{-/-}$ brain and $Mfp2^{-/-}$ microglia lacked signs of phagocytic and neurotoxic activity. The chronically reactive state of $Mfp2^{-/-}$ microglia was accompanied by downregulation of markers that specify the unique microglial signature in homeostatic conditions. In contrast, mammalian target of rapamycin (mTOR) and downstream glycolytic and protein translation pathways were induced, indicative of metabolic adaptations. $Mfp2^{-/-}$ microglia were immunologically activated but not polarized to a pro- or anti-inflammatory phenotype. A peripheral lipopolysaccharide challenge provoked an exaggerated inflammatory response in $Mfp2^{-/-}$ brain, consistent with a primed state. Taken together, we demonstrate that chronic activation of resident microglia does not necessarily lead to phagocytosis nor overt neurotoxicity.

Corresponding author: Myriam Baes, PhD, Laboratory for Cell Metabolism, Faculty of Pharmaceutical and Pharmacological Sciences, Campus Gasthuisberg O/N2, Herestraat 49, B 3000 Leuven, Tel + 32 16 330853, Fax + 32 16 330856, Myriam.Baes@pharm.kuleuven.be.
*Equal contribution

Keywords

Neuroinflammation; microglia; peroxisomes; phagocytosis

Introduction

Microglia, the resident immune cells of the CNS, are actively engaged in both homeostasis and pathology in the adult brain. Under physiological conditions, microglia constantly survey the microenvironment and communicate in a bidirectional way with neural cells (Ransohoff and Perry, 2009, Hughes, 2012, Gomez-Nicola et al., 2013, Prinz and Priller, 2014). It has become clear that microglia play a critical role in neuronal plasticity by controlling synaptic function and synaptogenesis (Tremblay et al., 2010, Salter and Beggs, 2014). Recently, important progress was made in the molecular characterization of homeostatic microglia, by differentiating their transcriptome signature from that of neural cells and other myeloid cells (Butovsky et al., 2012, Gautier et al., 2012, Chiu et al., 2013, Hickman et al., 2013, Butovsky et al., 2014).

In addition to their role in CNS homeostasis, microglia sense CNS damage and can act as versatile effector cells during neuropathological conditions. To this end, microglia adopt a range of activation states which remain ill-defined at the molecular level. In particular, the diverse phenotypes of microglia in conditions of chronic stress in the brain are poorly understood (Gomez-Nicola et al., 2013, Cherry et al., 2014). The morphological transition from ramified to amoeboid is accompanied by new effector functions that can vary widely and encompass proliferation, migration, production of cytokines and chemokines, and phagocytic activity. Whether chronically activated microglia always attain neurotoxic properties is still a matter of debate (Biber et al., 2014). An undervalued aspect in chronic neuroinflammation is that concomitant with acquiring novel shapes and functions, microglia might also lose features related to their homeostatic role. To better understand the spectrum of phenotypes of reactive microglia, information on gene expression and insights in signaling pathways are necessary. Recently, the microglia transcriptome of SOD1^{G93A} mice, an amyotrophic lateral sclerosis (ALS) model was defined (Butovsky et al., 2012, Chiu et al., 2013). These microglia concurrently upregulate both neurotoxic and neuroprotective factors as well as genes associated with lysosomal activity and phagocytosis (Chiu et al., 2013). Their molecular profile was different from that of lipopolysaccharide (LPS)-activated microglia and of M1 or M2 macrophages, and was denoted as a neurodegeneration-specific signature (Chiu et al., 2013).

Chronic microglia activation is an important hallmark of many neurodegenerative diseases and contributes significantly to the progression of these disorders (Glass et al., 2010). Moreover, microglial dysfunction might underlie some neurological disorders, such as Rett's syndrome (Derecki et al., 2013) and Nasu-Hakola disease (Satoh et al., 2011). Also in X-linked adrenoleukodystrophy, a neurometabolic disorder caused by peroxisomal β-oxidation deficiency (Kemp et al., 2012), microglia seem to play a pivotal role in disease pathogenesis. This is inferred from the therapeutic efficacy of bone marrow transplantation or hematopoietic stem cell gene therapy to halt the inflammatory demyelination seen in the

cerebral childhood form of the disease (ccALD) (Cartier et al., 2009, Cartier and Aubourg, 2010). Due to the absence of neuroinflammation in the corresponding mouse model (*Abcd1*−/−), the precise molecular abnormalities leading to cerebral inflammation and/or microglial dysfunction cannot be investigated (Kemp et al., 2012). Interestingly, we recently showed that mice lacking multifunctional protein-2 (MFP2; also known as D-bifunctional protein), a peroxisomal β-oxidation enzyme downstream of the ABCD1 transporter, develop robust neuroinflammation (Huyghe et al., 2006c, Verheijden et al., 2013). This initiates before the age of 8 weeks and is confined to the gray matter throughout the brain and spinal cord. The expanding inflammation parallels the aggravating neurological phenotype of the mice, characterized by motor and cognitive impairments, lethargy and death before the age of 6 months ((Huyghe et al., 2006c) and unpublished observations). With the exception of testicular degeneration, no peripheral organ failure was observed (Jia et al., 2003, Huyghe et al., 2006a, Huyghe et al., 2006b). Interestingly, mice with selective elimination of MFP2 from neural cells develop minor neuroinflammation and have an extended lifespan compared to general knockouts (Verheijden et al., 2013). This suggests that loss of peroxisomal β-oxidation from non-neural cells (e.g. microglia and/or infiltrating monocytes) worsens the inflammatory state of the brain.

For unknown reasons, the phenotype of *Mfp2*−/− mice deviates from the severe neurodevelopmental pathology of patients with total ablation of MFP2 (Ferdinandusse et al., 2006b). Milder mutations give rise to degenerative neurological anomalies including ataxia, leukodystrophy and vision/hearing problems (Ferdinandusse et al., 2006a, Khan et al., 2010, van der Knaap et al., 2012) but it has not been assessed whether neuroinflammation develops. The precise metabolic role of MFP2 in the formation and maintenance of the CNS remains unresolved. Apart from increased levels of very long chain fatty acids, no other metabolic anomalies have been identified (Huyghe et al., 2006a).

In this study, we used *Mfp2*−/− mice as a unique tool to study the cellular and molecular aspects of neuroinflammation in peroxisomal β-oxidation deficiency. Specifically, we aimed to molecularly define the activation state of microglia and to uncover the cellular mechanisms driving the neuroinflammatory response. Our findings show that *Mfp2*−/− microglia adopt a strongly proliferative and immunologically activated phenotype that is neuron-sparing. As this contrasts with microglia in the neurodegenerative milieu of the *SOD1*^{G93A} spinal cord (Chiu et al., 2013), we directly compared gene expression and histological features of microglia in both mouse models.

Materials and Methods

Mouse breeding

The generation of *Mfp2*−/− mice has been described (Baes et al., 2000). *Mfp2*−/− mice were bred on a Swiss/Webster background in the specific pathogen free animal housing facility of the KU Leuven, had *ad libitum* access to water and standard rodent food, and were kept on a 12-hour light and dark cycle. As we did not detect differences between wild type and heterozygous mice in our previous investigations, they were both used as controls. Unless stated otherwise, all experiments were performed on 17–20 week old mice with mixed gender and were in accordance with the "Guidelines for Care and Use of Experimental

Animals" and fully approved by the Research Ethical committee of the KU Leuven (#190/2012).

Microglia isolation by FACS sorting

Microglia were acutely isolated from *Mfp2*⁻/⁻ and control mice (n=4 for each genotype). After transcardiac perfusion with ice-cold PBS, brains were quickly dissected and mechanically homogenized with a tissue homogenizer in ice-cold HBSS containing 15mM HEPES and 0.5 % glucose (De Haas et al., 2007). Cells were filtered over a 70 μm strainer and pelleted at 220 g for 10 min at 4 °C. Contaminating myelin was removed by resuspending the pellet in 25 ml ice-cold 22% Percoll buffer, overlaying with 5 mL ice-cold PBS followed by centrifugation in a swinging bucket rotor at 950 g for 25 min at 4 °C (modified from (Olah et al., 2012)). The cells were incubated with mouse anti-CD45-FITC (eBiosciences 11–0451; 1:40) and mouse anti-CD11b-APC (eBiosciences 17–0112; 1:100) for 30 minutes at 4 °C in the dark. CD11b^high/CD45^mid cells were isolated using an Aria I fluorescence-activated cell sorter (FACS) (BD Biosciences) equipped with a 488 nm and 633 nm laser. Cells with low forward/sideward scatter profile were excluded from the isolation. Microglia yield ranged between 1×10^5 to 3×10^5 cells/mouse brain. Cells were collected in RNA lysis buffer provided with the RNeasy microkit (Qiagen, 74004). Data from FACS sorting of CD11b^high/CD45^mid myeloid cells were analyzed using BD FACsuite software (BD Biosciences).

Microarray

Total RNA was isolated from FACS sorted microglia by using the RNeasy Micro kit (Qiagen). The quality of the RNA samples was determined with an Agilent 2100 Bioanalyzer (Agilent Technologies, California, USA). Only samples with RIN values (RNA Integrity Number) higher or equal to 8 were used. The RNA was amplified with the NuGEN amplification kit (Agilent technologies). For microarray analysis, the whole genome GeneChip Mouse Gene 1.0 ST Array was used as described previously. Quality control, amplification, labeling of the samples, hybridization, washing and scanning of the chips and first-line bioinformatics was carried out at the MicroArray Facility (MAF, VIB, Leuven, Belgium). The complete dataset is available under GEO record GSE66420.

Flow cytometry

Brain cells were isolated by Percoll gradient centrifugation as described above. For antibody labeling, 1×10^5 cells were incubated in 200 μl for 20 min at 4 °C with combinations of mouse anti-Cd11b-APC (1:200) and either rat anti-LY6C-FITC (1:200), rat anti-5E12 (CD39) (1:300) rat anti-FCRLS (1:300) antibodies (Butovsky et al., 2012, Butovsky et al., 2014). The latter two were detected with goat anti-rat IgG conjugated to FITC (1:300; BioLegend). To demonstrate cell proliferation, bromodeoxyuridine (BrdU) (Sigma B5002) was dissolved in sterile Dulbecco's phosphate buffered saline at 37°C and injected intraperitoneally (50 mg/kg body weight) daily for 3 consecutive days in 12-week-old or 16-week-old *Mfp2* knockout and wild type littermates. Twelve hours after the last BrdU injection, proliferating cells were detected using flow cytometry with anti-BrDU antibodies (BrDU Flow Kit; BD Biosciences). Alternatively, animals were sacrificed for immunohistochemical detection of BrdU. Flow cytometry was performed on a FACSVerse

(BD Biosciences), and data analyzed with BD FACsuite software (BD Biosciences). For immunological profiling, CD11b-Pe Cy7 (clone M1/70, Biolegend) was used in combination with CD11c-APC (clone HL3, BD Pharmingen), F4/80-APC (clone BM8, eBioscience), CX3CR1-FITC (Goat polyclonal, R&D Systems), CD204-Alexa 647 (clone MR5D3, AbD Serotec), CD206-Alexa 647 (clone 2F8, AbD Serotec) or IL10R (Imtec Diagnostics) all at dilutions of 1:200.

Real time PCR

Real time PCR was performed as previously described (Bottelbergs et al., 2010) using an ABI PRISM 7500 Real Time PCR instrument (Applied Biosystems, Lennik, Belgium). Primers and probes were either designed using Primer Express Software (Applied Biosystems) (β-actin, iNOS, Tnf sequences available on request) or ordered from Applied Biosystems as premade Taqman Gene Expression assays (Il1b, Mm011336189_m1; Il6, Mm01210733_m1; Cx3cr1, Mm0262011_s1; Tgfbr1, Mm00436964_m1; arginase, Mm00475991_m1; Mrc1, Mm00485148_m1). Assays were performed in duplicate or triplicate in 10 μL TaqMan Fast Universal PCR Master Mix (Applied Biosystems). Relative expression levels of the target genes were calculated taking into account the amplification efficiency as described (Giulietti et al., 2001). The relative expression levels of the target genes were calculated as a ratio to the housekeeping gene β-actin.

Bioinformatics

Differential expression of genes between the two conditions is based on the robust multi-array analysis (RMA) expression values (Irizarry et al., 2003) as obtained with the xps package (version 1.18.1) of BioConductor (www.bioconductor.org). We tested whether it significantly deviates from 0 with a moderated t-statistic (implemented in limma). The resulting p-values are corrected for multiple testing with Benjamini-Hochberg (Hochberg and Benjamini, 1990) to control the false discovery rate. In general, differential expression is based on the p-values, corrected for multiple testing (e.g. all probes with a corrected p-value less than 0.01) together with a cut-off on the fold-change of 1.5. Pathway analysis is based on information provided by The Ingenuity Knowledge Base. For data interpretation and visualization Ingenuity pathway analysis (IPA) and the functional annotation tool KEGG (Kyoto Encyclopedia for Genes and Genomes database) from DAVID (Database for Annotation, Visualization and Integrated Discovery v6.7) was used. In addition, the dataset from $Mfp2^{-/-}$ microglia was compared to transcriptomics datasets based on either RNA-sequencing of microglia in homeostatic conditions and from SOD1^{G93A} mice (Chiu et al., 2013) (GEO dataset GSE43366) or gene expression profiling of microglia in homeostatic conditions using a NanoString nCounter platform (Butovsky et al., 2014). The RPKM gene levels from the RNA-seq experiment were converted to fold change as compared to control values. Differentially expressed genes (fold > 1.5, p-value < 0.01) were used for all analyses.

Histology

Anesthesia of the mice and tissue processing and immunohistochemical (IHC) staining were performed as described (Hulshagen et al., 2008). Routinely, paraffin sections (7 μm) were used for immunofluorescent stainings. The following primary antibodies were used: polyclonal rabbit anti-Iba1 (1:500; Wako D19–19741), rabbit anti-phospho-S6 ribosomal

protein mAb (Ser235/236) (1:400; Cell signaling D57.2.2E), rabbit Cathepsin D (1:200 Santa Cruz), Lamp2/Mac3 (1:100, BD Pharmingen), rat Anti-BrDU mAb (1:100; AbD Serotec OBT0030), rabbit 3-nitrotyrosine (1:100; Millipore 06–284), and rabbit 4-hydroxynonenal (1:500; Millipore 393204). Cryo sections were used for staining with polyclonal rabbit anti-P2RY12 (1:500; provided by Prof. O. Butovsky, Boston, USA). Frozen sections of spinal cord of endstage SOD1^{G93A} mice were kindly provided by Prof. L. Van Den Bosch (VIB and KU Leuven, Belgium). After incubation with primary antibodies overnight at room temperature (at 4°C for anti-P2RY12 staining) HRP-labeled secondary antibodies (1:200) were applied for 1 hour, followed by fluorescent labeling with a cyanine 2 (FITC) TSA kit (Perkin Elmer Life sciences, Boston, USA). P2ry12 antibodies were detected with goat anti-rabbit IgG conjugated to Alexa647 (1:300; Life technologies A21244). When double immunolabeling was performed, sets of primary and secondary antibodies were applied sequentially. As second fluorescent labels, cyanine 3 TSA kits (Perkin-Elmer) were used. Images were acquired with a motorized inverted IX-81 microscope connected to a CCD-FV2T digital camera (Olympus, Aartselaar, Belgium) and processed with LSM Image browser software (Zeiss, Germany). Microglia cell numbers were quantified on Iba-1 immunofluorescent stained paraffin sections (7 μm) around the sagittal midline (n=4). Within one plane (20 × magnification), only Iba-1-positive cells that fully colocalized with DAPI-positive nuclei were counted in the different regions of the brain, namely cornu ammonis (CA) 1–3 and dentate gyrus (DG) of hippocampus, somatosensory cortex, motor cortex and dorsal pons. Microglia number/frame was corrected for surface area. Quantification of neuronal numbers in CA3 of hippocampus was performed on cresyl violet stained sections (n=5) in a similar way as described for microglia. Only cells in which the Nissl substance was clearly visible were quantified.

In vivo LPS challenge and cytokine measurements

Mfp2$^{-/-}$ and control mice 14 weeks of age received an intraperitoneal injection of LPS (1mg/kg, Sigma, L4391) or sterile saline vehicle in a total volume of 100μl. Four hours later, mice were sacrificed, plasma and brain regions were collected and flash frozen in liquid nitrogen. Brainstem was homogenized 1:10 (w/v) in ice-cold PBS containing a cocktail of protease inhibitors (Roche) and lysates were cleared by centrifugation at 14000g for 20 min at 4°C. Immunoreactive levels of TNF, IL1β and IL6 were measured in plasma and brainstem lysates by using a cytometric bead array mouse soluble protein flex set system (BD Biosciences). The samples were prepared according to the manufacturer's instructions and analyzed on a FACSCanto HTS (BD Biosciences) and analyzed by FCAP array software (BD Biosciences).

Statistical analysis

One-way ANOVA was carried out using Graphpad Prism 3.0 software (San Diego, CA). For microarray data, p-values are corrected for multiple testing with Benjamini-Hochberg (Hochberg and Benjamini, 1990).

Results

No invasion of Ly6C⁺ monocytes but proliferation of resident microglia in *Mfp2⁻/⁻* brain

One of the most striking neuropathological hallmarks of *Mfp2⁻/⁻* mice is the development of extensive neuroinflammation involving astro- and microgliosis (Huyghe et al., 2006c, Verheijden et al., 2013). During the disease course, Iba1⁺ brain macrophages acquire an activated phenotype and display enlarged cell bodies and a deramified morphology together with increased F4/80 expression (Verheijden et al., 2013). In order to estimate whether these cells increase in number, Iba1⁺ cells were quantified in different regions of the CNS of mice at end stage (5 months old). In hippocampus, motor cortex and pons, microglia/macrophage numbers were 4–6 fold increased in *Mfp2⁻/⁻* compared to control brain (Fig. 1A). To investigate whether this increase arises from influx of peripheral monocytes or accumulation of resident microglia, we evaluated the presence of markers that are respectively expressed by blood monocytes (Ly6C) and resident microglia (CD39, FCRLS). Indeed, *Butovsky et al* recently showed that the expression of Ly6C and CD39/FCRLS effectively distinguishes non-overlapping populations of peripheral inflammatory monocytes and CNS-resident microglia in mice (Butovsky et al, 2012; Butovsky et al, 2014). The efficacy of these discriminating markers has been convincingly proven in a mouse model of ALS (SOD1^{G93A})(Butovsky et al., 2012, Butovsky et al., 2014). FACS analysis on brain homogenates of endstage *Mfp2⁻/⁻* mice showed that almost all CD11b⁺ cells are negative for the monocyte marker Ly6C (> 99%) (Fig.1B). In contrast, the vast majority of CD11b⁺ cells (> 97%) is positive for CD39 and FCRLS, two specific markers for resident microglia (Fig. 1C–D). Moreover, all CD11b⁺ cells are CD45^{dim}, which is another characteristic of resident microglia (data not shown). Together, these data show that the expanded myeloid population is of local origin allowing to further designate these cells as microglia.

Having excluded influx of inflammatory monocytes in the *Mfp2⁻/⁻* brain, we next wanted to verify whether the accumulation of brain myeloid cells originates from proliferation of CNS resident microglia. We analyzed BrdU incorporation in microglial cells and indeed found significantly increased numbers of proliferating Iba1⁺/BrdU⁺ cells by IHC analysis (Fig. 1E) and Cd11b⁺/BrdU⁺ cells by FACS analysis in *Mfp2⁻/⁻* compared to control mice (Fig. 1F,G). Together, these data demonstrate that the inflammatory response in *Mfp2⁻/⁻* brain is governed by proliferation of resident microglia and not by infiltration of peripheral cells.

Defining the molecular signature of a non-neurodegenerative microglia phenotype

As microgliosis in *Mfp2⁻/⁻* mice is confined to gray matter areas such as cortex, hippocampus and brainstem (Verheijden et al., 2013), we performed double immunofluorescence stainings with microglial and neuronal markers. We observed that microglia enwrap neuronal cell bodies (Fig. 2A–F), suggesting that microglia in *Mfp2⁻/⁻* mice become activated in response to neuronal demise, analogous to several disease models of neurodegenerative disorders. However, previous FluoJade and caspase/TUNEL stainings did not show evidence for neuronal damage nor death in the CNS of *Mfp2⁻/⁻* mice (Huyghe et al., 2006c). To further confirm the conservation of neurons, we counted neuron numbers in the CA3 region of the hippocampus of endstage *Mfp2⁻/⁻* mice (Fig. 2G–I). We did not find significant differences between *Mfp2⁻/⁻* and control mice. Also in other brain regions,

we could not detect an overt reduction of neuron numbers (not shown). The microglia microenvironment in *Mfp2*^{−/−} brain thus deviates from the milieu in neurodegenerative disorders. We therefore characterized the molecular signature of this non-neurodegenerative microglia phenotype and performed microarray analysis on acutely isolated microglia (CD11b$^+$/CD45^{dim}) from whole brain of 5 months old control and *Mfp2*^{−/−} mice (Fig. 3A,B). We found that 983 genes were differentially expressed in *Mfp2*^{−/−} compared to control microglia (288 downregulated, 695 upregulated; fold 1.5, p-value < 0.01) (Fig. 3C). The top 50 up- and downregulated genes, the unsupervised hierarchical clustering of RMA values and the principle component analysis of gene expression data are shown in Suppl. Fig.1. Pathway enrichment by Ingenuity and DAVID analysis demonstrated pronounced induction of pathways related to protein translation, cellular growth and proliferation, such as *Eif2 signaling*, *mTOR signaling* and *regulation of eIF4 and p70S6K signaling* (Fig. 3D and Suppl. Table 1). Activation of mTOR was validated by IHC, showing increased phosphorylation of the downstream target ribosomal S6 protein (pS6) in *Mfp2*^{−/−} compared to wild type microglia (Fig. 3E,F). The transcription factor Hypoxia-inducible factor 1-alpha (HIF1α), another downstream target of mTOR (Duvel et al., 2010), was significantly induced according to the microarray data, which was further supported by elevated transcripts of several enzymes of the glycolytic pathway and VEGF (Suppl. Table 1). Interestingly, the regulatory subunit of 5' AMP-activated protein kinase (AMPK) that inhibits mTOR in conditions of cellular energy depletion, was downregulated by 50%. The enrichment of mTOR and eIF2 signaling is in accordance with the strong proliferative response and cellular growth observed in *Mfp2*^{−/−} microglia.

Microglia in *Mfp2*^{−/−} brain are not phagocytic and do not produce reactive oxygen/nitrogen species

We compared the transcriptional signature of *Mfp2*^{−/−} microglia residing in a neuron-sparing milieu, with the previously published neurodegeneration-specific microglial signature in *SOD1*^{G93A} mice, a model for ALS (GEO dataset GSE43366)(Chiu et al., 2013). The most pronounced difference between the *Mfp2*^{−/−} and *SOD1*^{G93A} model was the strong enrichment of the KEGG pathway *Lysosome* in *SOD1*^{G93A} microglia (37.9% of genes related to *Lysosome* upregulated) (Fig. 4B) whereas this was less obvious for *Mfp2*^{−/−} microglia (11.7% of genes upregulated) (Fig. 4A). Comparison for enriched functions between the two models using Ingenuity analysis demonstrated marked enrichment for 'phagocytosis', 'cytoskeletal organization' and 'respiratory burst' in the *SOD1*^{G93A} as compared to *Mfp2*^{−/−} microglia (Fig. 4C). As these data suggest that microglia in *Mfp2*^{−/−} mice do not acquire phagocytic properties, in contrast to microglia in a neurodegenerative disease model (*SOD1*^{G93A}), we performed IHC for markers associated with lysosomal activation and phagocytosis. There was no increased immunoreactivity of Cathepsin D (Fig. 4D,E), LAMP2/MAC3 (Fig. 4G,H) and CD68 (not shown) in brain of *Mfp2*^{−/−} versus control mice (shown for visual cortex and brainstem). In contrast, we detected clear positive staining for these markers in the lumbal spinal cord of endstage *SOD1*^{G93A} mice (Fig. 4F,I).

The low expression of 'respiratory burst' genes in *Mfp2*^{−/−} as compared to *SOD1*^{G93A} microglia comprised normal levels of *Nos2*, *Nox1* and *Nox2* (*Cybb*) versus controls. In contrast, *SOD1*^{G93A} microglia showed a very strong upregulation of *Cybb* compared to

control microglia (> 40 fold) (Chiu et al., 2013). As reactive oxygen and nitrogen species are known to be important mediators of neurotoxicity, and upregulation might take place at the posttranscriptional level, we further evaluated oxidative stress markers. IHC stainings for nitrated proteins (Fig. 4J–L) and lipid peroxidation (4HNE, not shown) were not detectable in *Mfp2*$^{-/-}$ brain (Fig. 4K), whereas both were positive in *SOD1*^{G93A} spinal cord (Fig. 4L and data not shown).

In summary, despite their chronic active state, *Mfp2*$^{-/-}$ microglia do not upregulate pathways associated with phagocytic clearance, lysosomal activity and reactive oxygen/ nitrogen species production. This is in striking contrast to the neurodegeneration-specific microglial signature of *SOD1*^{G93A} mice.

Mfp2$^{-/-}$ microglia are immunologically activated but not polarized

In response to disruption of CNS homeostasis by infectious or sterile conditions, reactive microglia can produce pro-inflammatory cytokines such as TNF. Chronic release of these substances by microglia can affect neuronal viability (Block et al., 2007). In contrast, the induction of an anti-inflammatory microglia phenotype is generally linked to neuroprotection (Kigerl et al., 2009, Liao et al., 2012). In view of preserved neuron numbers in *Mfp2*$^{-/-}$ mice and the absence of a neurodegeneration-specific microglial signature, we explored transcript levels of genes associated with pro- and anti-inflammatory activation in the micro-array dataset. Microglia in *Mfp2*$^{-/-}$ mice are clearly immunologically activated as several genes encoding cytokines (*Il1b, Tnf, Il12b*), chemokines (*Ccl5, Ccl2*) and surface markers (*Itgax, Emr1, Cd83, Cd86*) associated with inflammatory activation were strongly induced (Fig. 5A,C). Remarkably, the expression of several key pro-inflammatory genes was unchanged (*Nos2, Il12a, Cxcl9, Ifnb1, Icam1*) or even downregulated (*Il6*), suggesting that microglia in *Mfp2*$^{-/-}$ mice do not acquire a typical pro-inflammatory activation state. However, *Mfp2*$^{-/-}$ microglia could also not be categorized as anti-inflammatory, because typical anti-inflammatory genes were either induced (*Arg1, Msr1*) or repressed (*Mrc1, Stab1*) (Fig. 5A–C). qRT-PCR and FACS analysis of some key inflammatory markers further confirmed that the microglia activation state in *Mfp2*$^{-/-}$ mice cannot be categorized as pro- or anti-inflammatory (Fig. 5B,D). Analysis of cytokine levels in brain homogenates revealed that despite strongly increased transcript levels of *Tnf* and *Il1b* in microglia, the respective cytokine levels were not detectable (TNF) or only 1.5 fold increased (IL1β) (not shown) in *Mfp2*$^{-/-}$ brain, further supporting the absence of a typical pro-inflammatory effector state. Interestingly, after intraperitoneal injection of LPS, both transcript (Tnf, Il1b) and protein levels (IL1β, IL6 and TNFα) were more strongly induced in *Mfp2*$^{-/-}$ compared to control mice, consistent with a primed state (Perry and Holmes, 2014) (Fig. 5E,F). In order to exclude that this particular immunological state of microglia is induced by systemic inflammation, we analyzed cytokine levels in plasma (Il1β, Il6, TNFα) and the leucocyte profile in blood. There were however no signs of peripheral inflammatory anomalies in *Mfp2*$^{-/-}$ mice and after LPS administration cytokine levels increased similarly in control and mutant mice (data not shown).

It thus seems that *Mfp2⁻/⁻* microglia exhibit an immunologically activated and primed state, but they are not polarized and only acquire a typical pro-inflammatory effector state after a secondary stimulus.

The homeostatic microglial signature is downregulated in *Mfp2⁻/⁻* microglia

Several research groups recently reported the specific transcript signature of homeostatic microglia (Gautier et al., 2012, Chiu et al., 2013, Hickman et al., 2013, Butovsky et al., 2014) by comparing the transcriptomes of microglia with those of other CNS cell types and/or peripheral myeloid cells. This resulted in the identification of specific markers of microglia in their surveillance mode. When comparing our data set with the homeostatic microglial signature, it was conspicuous that the bulk of microglia specific genes was significantly suppressed in *Mfp2⁻/⁻* microglia (46% when compared with Butovsky et al. (Butovsky et al., 2014) (Fig. 6A) and 53 % compared with Chiu et al. (Chiu et al., 2013)), whereas only a few were upregulated (6–9%). These data demonstrate that in the inflamed *Mfp2⁻/⁻* brain, microglia loose typical features related to their homeostatic function. In order to validate the microarray data, we performed qRT-PCR of *Cx3cr1* and *Tgfbr1* on isolated microglia (Fig. 6B,C) and IHC analysis of P2RY12 (Fig. 6D,E) which confirmed the downregulation of these surface markers in *Mfp2⁻/⁻* microglia. FACS analysis for CX3CR1 and IL10R showed a clear reduction in CX3CR1 expression and a slight reduction in IL10R expression (Fig. 6F,G). Taken together, a hallmark of the microglia phenotype in *Mfp2⁻/⁻* brain is the loss of surface and other markers that were shown to be highly and exclusively expressed in these cells in homeostatic conditions.

Discussion

This study contributes to a better understanding of the wide spectrum of phenotypes that microglia can adopt in the diseased brain. We determined the microglial signature in a murine model of peroxisomal β-oxidation deficiency in which robust and chronic inflammation in the gray matter occurs in the absence of neuronal loss. We show that the resident microglia in *Mfp2⁻/⁻* mice proliferate, are permanently in an activated non-phagocytic state and lose their typical homeostatic markers. Our data prove that microglia can remain in a reactive state without acquiring overt neurotoxic and phagocytic properties.

As infiltrating bone marrow-derived monocytes may have a major impact on the pathological course of neurological conditions (Prinz and Mildner, 2011, Yamasaki et al., 2014), it was of prime importance to establish the source of the expanded microglial compartment in *Mfp2⁻/⁻* mice. Analysis of specific markers corresponding to peripheral monocytes and resident microglia clearly showed that the myeloid cells in *Mfp2⁻/⁻* brain, even at late stages of disease, solely derive from local microglia. This differs from the neuroinflammatory demyelination condition in the peroxisomal β-oxidation disorder, ccALD in which the fast progressive phase coincides with opening of the blood brain barrier (Kemp et al., 2012).

Although the immunological profile of *Mfp2⁻/⁻* microglia is clearly distinct from naive microglia, the affected cytokines and inflammatory mediators could not be clustered in currently known pro- or anti-inflammatory states. In contrast to acute insults to the brain,

where microglia switch from an initial proinflammatory to a resolving anti-inflammatory state, the microglial phenotype in chronic sterile stress conditions can be very heterogeneous. In the $SOD1^{G93A}$ mouse model of ALS, microglia were shown to convert during the course of disease from an alternatively activated to a classically activated state (Liao et al., 2012). The latter were shown to be neurotoxic to motor neurons in vitro. It is now recognized that microglia induce inflammatory markers in the aged rodent brain and it is hypothesized that this modest chronic neuroinflammation impairs neuronal functioning (Norden and Godbout, 2013). Age is not contributing to the inflammatory response in our model as mice only survive up to 5–6 months of age. It remains however unsolved whether long-term activation of microglia is necessarily deleterious for neural cells (Biber et al., 2014). Interestingly, crucial players in the neurotoxic properties are reactive oxygen and nitrogen species (Block et al., 2007, Brown and Neher, 2014). Although a set of pro-inflammatory surface and cytokine markers are induced in $Mfp2^{-/-}$ microglia, the genes responsible for generation of reactive oxygen and nitrogen species are not upregulated, even at endstage of disease. The induction of $Arg1$, a well characterized anti-inflammatory marker gene, also indicates that $Mfp2^{-/-}$ microglia are rather protective for their environment than toxic. Indeed, the enzyme arginase 1 utilizes, similar to iNOS, arginine as a substrate, but converts it to products that serve as precursors in repair processes and not to destructive nitrogen species (Lange et al., 2004, Estevez et al., 2006).

Gene expression screening and histological analyses further indicated absence of lysosomal activity and cytoskeletal remodeling that normally accompany phagocytosis. This is in sharp contrast with the gene expression signature of $SOD1^{G93A}$ microglia in which these pathways were strongly induced (Chiu et al., 2013). In the latter model, microglia respond to early changes in motor neurons and develop phagocytic and neurotoxic properties even in a presymptomatic stage (Sanagi et al., 2010). On the contrary, reactive microglia in $Mfp2^{-/-}$ brain seem to get stuck in their graded response from a ramified to a fully activated phagocytic state. This raises the question whether $Mfp2^{-/-}$ microglia have the ability to develop lysosomal activity and execute phagocytosis. In this respect it is important to note that cathepsin D positive microglia were present in cerebellar white matter (data not shown), where we previously showed degeneration of Purkinje cell axons (Verheijden et al., 2013), indicative of a proper phagocytic function. Microglia in MFP2 deficient mice thus transform for a prolonged period in a reactive state that lacks neurodestructive behavior within their lifetime. It needs to be elucidated whether this state is triggered by cell autonomous processes in microglia resulting from peroxisomal β-oxidation inactivity or by microglial responses to MFP2 deficiency in neighbouring cells or a combination of these mechanisms. The fact that the microglial reactivity is confined to the gray matter strongly suggests that metabolic distress caused by peroxisomal MFP2 deficiency in neurons contributes to pathology.

In view of the seemingly harmless microglial activation, the question arises whether this contributes to disease pathogenesis in $Mfp2^{-/-}$ mice as increasing microgliosis coincides with the neurological symptoms. In this respect, it should be emphasized that the most prominent coordinated change in $Mfp2^{-/-}$ microglia is rather a loss-of-function than a toxic-gain-of-function. Several research groups recently defined the unique transcriptome signature of homeostatic microglia by comparison with their neural cell neighbors and

myeloid cell family members (Gautier et al., 2012, Chiu et al., 2013, Hickman et al., 2013, Butovsky et al., 2014). These typical microglial markers were generally downregulated in *Mfp2−/−* microglia pointing to a loss of their surveillance state. Butovsky et al recently reported that the microglia specific gene signature is mainly driven by transforming growth factor β (TGFβ) and that loss of TGFβ signaling leads to downregulation of the homeostatic gene signature (Butovsky et al., 2014). In *Mfp2−/−* microglia the expression of *Tgbr1* was downregulated, probably contributing to their loss-of-homeostatic-function phenotype. A large fraction of the downregulated genes encode cell surface proteins such as the purinergic receptors P2RY12 and P2RY13. It should however be noted that this loss of microglial membrane proteins is selective as several others are either unchanged (e.g. P2RY6) or increased (e.g. P2RX4) in expression. It is plausible that these alterations will perturb the microglial communication with the microenvironment or that chronic deprivation of homeostatic microglial properties impairs neurological function. It was indeed shown that lack of CX3CR1 signaling in microglia perturbs synaptic function in the postnatal period resulting in persistently disturbed brain connectivity and behavioral disorders (Zhan et al., 2014). Furthermore, loss of microglia in adulthood was proven to impact on memory and motor learning through impaired synapse formation, emphasizing the importance of proper neuron-microglia crosstalk in normal brain functioning (Parkhurst et al., 2013).

Whereas the primary trigger for microglia activation in *Mfp2−/−* brain remains unknown, we found that mTOR and other pathways driving protein synthesis were induced in the reactive microglia. Activation of these pathways leads to cell proliferation and growth, in line with the observed morphological and mitogenic response of *Mfp2−/−* microglia. The pathways downstream of mTOR are known to be involved in ribosomal activity, protein synthesis and energy generation through induction of HIF1α, glycolysis, and enhanced mitochondrial functioning (Hay and Sonenberg, 2004, Duvel et al., 2010). In fact, little is known on the role of mTOR in the diverse microglial phenotypes. *In vitro* experiments with primary microglia and BV2 cells showed increased mTOR signaling after exposure to hypoxia, LPS or a mixture of cytokines (Lu et al., 2006). Mouse models with various neurological conditions such as spinal cord injury and epilepsy, were shown to improve when treated with mTOR inhibitors but the impact on the inflammatory reaction remains poorly documented (Sekiguchi et al., 2012, van Vliet et al., 2012, Lu et al., 2014). Interestingly, mTOR was recently identified as a novel factor involved in macrophage polarization although contradictory findings were reported whether mTOR activation biases the cytokine response towards a pro- or an anti-inflammatory state (Byles et al., 2013, Luo et al., 2014). In addition, it was recently shown that the AKT-mTOR-HIF1α pathway is instrumental for 'training' of macrophages whereby cytokine expression is enhanced following a prior exposure to β-glycan (Cheng et al., 2014, Saeed et al., 2014). This signaling orchestrates a switch in macrophages from oxidative metabolism to aerobic glycolysis. In this respect, the upregulation of the mTOR pathway in *Mfp2−/−* microglia, may play a broader role than only sustain growth and proliferation. The activation of the transcription factor HIF1α and its downstream glycolytic enzymes might play a pivotal role in the primed state of *Mfp2−/−* brain and possibly in other chronic neuroinflammatory states. In view of the premise that primed microglia in neurodegenerative diseases become detrimental after a systemic insult such as infection or illness, it is important to further investigate whether targeting mTOR can

modify the microglia expression pattern in *Mfp2*$^{-/-}$ mice and in other neuroinflammatory conditions.

In conclusion, our data indicate that chronically reactive microglia in *Mfp2*$^{-/-}$ brain adopt an immunologically activated but non-polarized phenotype that is marked by morphological and metabolic adaptations. These microglia act in a pro-survival environment without overt neuronal demise, although an adverse effect on neuronal functioning through loss of microglial homeostatic functions cannot be excluded.

Supplementary Material

Refer to Web version on PubMed Central for supplementary material.

Acknowledgments

References

Baes M, Huyghe S, Carmeliet P, Declercq PE, Collen D, Mannaerts GP, Van Veldhoven PP. 2000 Inactivation of the peroxisomal multifunctional protein-2 in mice impedes the degradation of not only 2-methyl branched fatty acids and bile acid intermediates but also of very long chain fatty acids. J Biol Chem 275:16329–16336. [PubMed: 10748062]

Biber K, Owens T, Boddeke E. 2014 What is microglia neurotoxicity (Not)? Glia 62:841–854. [PubMed: 24590682]

Block ML, Zecca L, Hong JS. 2007 Microglia-mediated neurotoxicity: uncovering the molecular mechanisms. Nat Rev Neurosci 8:57–69. [PubMed: 17180163]

Bottelbergs A, Verheijden S, Hulshagen L, Gutmann DH, Goebbels S, Nave KA, Kassmann C, Baes M. 2010 Axonal integrity in the absence of functional peroxisomes from projection neurons and astrocytes. Glia 58:1532–1543. [PubMed: 20578053]

Brown GC, Neher JJ. 2014 Microglial phagocytosis of live neurons. Nat Rev Neurosci 15:209–216. [PubMed: 24646669]

Butovsky O, Jedrychowski MP, Moore CS, Cialic R, Lanser AJ, Gabriely G, Koeglsperger T, Dake B, Wu PM, Doykan CE, Fanek Z, Liu L, Chen Z, Rothstein JD, Ransohoff RM, Gygi SP, Antel JP, Weiner HL. 2014 Identification of a unique TGF-beta-dependent molecular and functional signature in microglia. Nat Neurosci 17:131–143. [PubMed: 24316888]

Butovsky O, Siddiqui S, Gabriely G, Lanser AJ, Dake B, Murugaiyan G, Doykan CE, Wu PM, Gali RR, Iyer LK, Lawson R, Berry J, Krichevsky AM, Cudkowicz ME, Weiner HL. 2012 Modulating inflammatory monocytes with a unique microRNA gene signature ameliorates murine ALS. J Clin Invest 122:3063–3087. [PubMed: 22863620]

Byles V, Covarrubias AJ, Ben-Sahra I, Lamming DW, Sabatini DM, Manning BD, Horng T. 2013 The TSC-mTOR pathway regulates macrophage polarization. Nat Commun 4:2834. [PubMed: 24280772]

Cartier N, Aubourg P. 2010 Hematopoietic stem cell transplantation and hematopoietic stem cell gene therapy in X-linked adrenoleukodystrophy. Brain Pathology 20:857–862. [PubMed: 20626747]

Cartier N, Hacein-Bey-Abina S, Bartholomae CC, Veres G, Schmidt M, Kutschera I, Vidaud M, Abel U, Dal-Cortivo L, Caccavelli L, Mahlaoui N, Kiermer V, Mittelstaedt D, Bellesme C, Lahlou N, Lefrere F, Blanche S, Audit M, Payen E, Leboulch P, l'Homme B, Bougneres P, Von KC, Fischer

A, Cavazzana-Calvo M, Aubourg P. 2009 Hematopoietic stem cell gene therapy with a lentiviral vector in X-linked adrenoleukodystrophy. Science 326:818–823. [PubMed: 19892975]

Cheng SC, Quintin J, Cramer RA, Shepardson KM, Saeed S, Kumar V, Giamarellos-Bourboulis EJ, Martens JH, Rao NA, Aghajanirefah A, Manjeri GR, Li Y, Ifrim DC, Arts RJ, van der Veer BM, Deen PM, Logie C, O'Neill LA, Willems P, van de Veerdonk FL, van der Meer JW, Ng A, Joosten LA, Wijmenga C, Stunnenberg HG, Xavier RJ, Netea MG. 2014 mTOR- and HIF-1alpha-mediated aerobic glycolysis as metabolic basis for trained immunity. Science 345:1250684. [PubMed: 25258083]

Cherry JD, Olschowka JA, O'Banion MK. 2014 Neuroinflammation and M2 microglia: the good, the bad, and the inflamed. J Neuroinflammation 11:98. [PubMed: 24889886]

Chiu IM, Morimoto ET, Goodarzi H, Liao JT, O'Keeffe S, Phatnani HP, Muratet M, Carroll MC, Levy S, Tavazoie S, Myers RM, Maniatis T. 2013 A neurodegeneration-specific gene-expression signature of acutely isolated microglia from an amyotrophic lateral sclerosis mouse model. Cell Rep 4:385–401. [PubMed: 23850290]

De Haas AH, Boddeke HW, Brouwer N, Biber K. 2007 Optimized isolation enables ex vivo analysis of microglia from various central nervous system regions. Glia 55:1374–1384. [PubMed: 17661344]

Derecki NC, Cronk JC, Kipnis J. 2013 The role of microglia in brain maintenance: implications for Rett syndrome. Trends Immunol 34:144–150. [PubMed: 23122051]

Duvel K, Yecies JL, Menon S, Raman P, Lipovsky AI, Souza AL, Triantafellow E, Ma Q, Gorski R, Cleaver S, Vander Heiden MG, MacKeigan JP, Finan PM, Clish CB, Murphy LO, Manning BD. 2010 Activation of a metabolic gene regulatory network downstream of mTOR complex 1. Mol Cell 39:171–183. [PubMed: 20670887]

Estevez AG, Sahawneh MA, Lange PS, Bae N, Egea M, Ratan RR. 2006 Arginase 1 regulation of nitric oxide production is key to survival of trophic factor-deprived motor neurons. J Neurosci 26:8512–8516. [PubMed: 16914676]

Ferdinandusse S, Denis S, Mooyer PA, Dekker C, Duran M, Soorani-Lunsing RJ, Boltshauser E, Macaya A, Gartner J, Majoie CB, Barth PG, Wanders RJ, Poll-The BT. 2006a Clinical and biochemical spectrum of D-bifunctional protein deficiency. Ann Neurol 59:92–104. [PubMed: 16278854]

Ferdinandusse S, Denis S, Mooyer PAW, Dekker C, Duran M, Soorani-Lunsing RJ, Boltshauser E, Macaya A, G,,rtner J, Majoie CBLM, Barth PG, Wanders RJA, Poll-The BT. 2006b Clinical and biochemical spectrum of D-bifunctional protein deficiency. Ann Neurol 59:92–104. [PubMed: 16278854]

Gautier EL, Shay T, Miller J, Greter M, Jakubzick C, Ivanov S, Helft J, Chow A, Elpek KG, Gordonov S, Mazloom AR, Ma'ayan A, Chua WJ, Hansen TH, Turley SJ, Merad M, Randolph GJ. 2012 Gene-expression profiles and transcriptional regulatory pathways that underlie the identity and diversity of mouse tissue macrophages. Nat Immunol 13:1118–1128. [PubMed: 23023392]

Giulietti A, Overbergh L, Valckx D, Decallonne B, Bouillon R, Mathieu C. 2001 An overview of realtime quantitative PCR: applications to quantify cytokine gene expression. Methods 25:386–401. [PubMed: 11846608]

Glass CK, Saijo K, Winner B, Marchetto MC, Gage FH. 2010 Mechanisms underlying inflammation in neurodegeneration. Cell 140:918–934. [PubMed: 20303880]

Gomez-Nicola D, Fransen NL, Suzzi S, Perry VH. 2013 Regulation of microglial proliferation during chronic neurodegeneration. J Neurosci 33:2481–2493. [PubMed: 23392676]

Hay N, Sonenberg N. 2004 Upstream and downstream of mTOR. Genes Dev 18:1926–1945. [PubMed: 15314020]

Hickman SE, Kingery ND, Ohsumi TK, Borowsky ML, Wang LC, Means TK, El Khoury J. 2013 The microglial sensome revealed by direct RNA sequencing. Nat Neurosci 16:1896–1905. [PubMed: 24162652]

Hochberg Y, Benjamini Y. 1990 More powerful procedures for multiple significance testing. Stat Med 9:811–818. [PubMed: 2218183]

Hughes V 2012 Microglia: The constant gardeners. Nature 485:570–572. [PubMed: 22660301]

Hulshagen L, Krysko O, Bottelbergs A, Huyghe S, Klein R, Van Veldhoven PP, De Deyn PP, D'Hooge R, Hartmann D, Baes M. 2008 Absence of functional peroxisomes from mouse CNS causes dysmyelination and axon degeneration. J Neurosci 28:4015–4027. [PubMed: 18400901]

Huyghe S, Mannaerts GP, Baes M, Van Veldhoven PP. 2006a Peroxisomal multifunctional protein-2: the enzyme, the patients and the knockout mouse model. BBA Mol Cell Biol L 1761:973–994.

Huyghe S, Schmalbruch H, De Gendt K, Verhoeven G, Guillou F, Van Veldhoven PP, Baes M. 2006b Peroxisomal multifunctional protein 2 is essential for lipid homeostasis in Sertoli cells and for male fertility in mice. Endocrinology 147:2228–2236. [PubMed: 16484321]

Huyghe S, Schmalbruch H, Hulshagen L, Van Veldhoven PP, Baes M, Hartmann D. 2006c Peroxisomal multifunctional protein-2 deficiency causes motor deficits and glial lesions in the adult CNS. Am J Pathology 168:1321–1334.

Irizarry RA, Hobbs B, Collin F, Beazer-Barclay YD, Antonellis KJ, Scherf U, Speed TP. 2003 Exploration, normalization, and summaries of high density oligonucleotide array probe level data. Biostatistics 4:249–264. [PubMed: 12925520]

Jia Y, Qi C, Zhang Z, Hashimoto T, Rao MS, Huyghe S, Suzuki Y, Van Veldhoven PP, Baes M, Reddy JK. 2003 Overexpression of peroxisome proliferator-activated receptor-alpha (PPARalpha)-regulated genes in liver in the absence of peroxisome proliferation in mice deficient in both L- and D- forms of enoyl-CoA hydratase/dehydrogenase enzymes of peroxisomal beta-oxidation system. J Biol Chem 278:47232–47239. [PubMed: 14500732]

Kemp S, Berger J, Aubourg P. 2012 X-linked adrenoleukodystrophy: metabolic, genetic and clinical aspects. BBA-Mol Basis Dis 1822:1465–1474.

Khan A, Wei XC, Snyder FF, Mah JK, Waterham H, Wanders RJ. 2010 Neurodegeneration in D-bifunctional protein deficiency: diagnostic clues and natural history using serial magnetic resonance imaging. Neuroradiology 52:1163–1166. [PubMed: 20848092]

Kigerl KA, Gensel JC, Ankeny DP, Alexander JK, Donnelly DJ, Popovich PG. 2009 Identification of two distinct macrophage subsets with divergent effects causing either neurotoxicity or regeneration in the injured mouse spinal cord. J Neurosci 29:13435–13444. [PubMed: 19864556]

Lange PS, Langley B, Lu P, Ratan RR. 2004 Novel roles for arginase in cell survival, regeneration, and translation in the central nervous system. J Nutr 134:2812S–2817S. [PubMed: 15465791]

Liao B, Zhao W, Beers DR, Henkel JS, Appel SH. 2012 Transformation from a neuroprotective to a neurotoxic microglial phenotype in a mouse model of ALS. Exp Neurol 237:147–152. [PubMed: 22735487]

Lu DY, Liou HC, Tang CH, Fu WM. 2006 Hypoxia-induced iNOS expression in microglia is regulated by the PI3-kinase/Akt/mTOR signaling pathway and activation of hypoxia inducible factor-1alpha. Biochem Pharmacol 72:992–1000. [PubMed: 16919605]

Lu Q, Gao L, Huang L, Ruan L, Yang J, Huang W, Li Z, Zhang Y, Jin K, Zhuge Q. 2014 Inhibition of mammalian target of rapamycin improves neurobehavioral deficit and modulates immune response after intracerebral hemorrhage in rat. J Neuroinflammation 11:44. [PubMed: 24602288]

Luo L, Wall AA, Yeo JC, Condon ND, Norwood SJ, Schoenwaelder S, Chen KW, Jackson S, Jenkins BJ, Hartland EL, Schroder K, Collins BM, Sweet MJ, Stow JL. 2014 Rab8a interacts directly with PI3Kgamma to modulate TLR4-driven PI3K and mTOR signalling. Nat Commun 5:4407. [PubMed: 25022365]

Norden DM, Godbout JP. 2013 Review: microglia of the aged brain: primed to be activated and resistant to regulation. Neuropathol Appl Neurobiol 39:19–34. [PubMed: 23039106]

Olah M, Raj D, Brouwer N, De Haas AH, Eggen BJ, Den Dunnen WF, Biber KP, Boddeke HW. 2012 An optimized protocol for the acute isolation of human microglia from autopsy brain samples. Glia 60:96–111. [PubMed: 21989594]

Parkhurst CN, Yang G, Ninan I, Savas JN, Yates JR 3rd, Lafaille JJ, Hempstead BL, Littman DR, Gan WB. 2013 Microglia promote learning-dependent synapse formation through brain-derived neurotrophic factor. Cell 155:1596–1609. [PubMed: 24360280]

Perry VH, Holmes C. 2014 Microglial priming in neurodegenerative disease. Nat Rev Neurol 10:217–224. [PubMed: 24638131]

Prinz M, Mildner A. 2011 Microglia in the CNS: immigrants from another world. Glia 59:177–187. [PubMed: 21125659]

Prinz M, Priller J. 2014 Microglia and brain macrophages in the molecular age: from origin to neuropsychiatric disease. Nat Rev Neurosci 15:300–312. [PubMed: 24713688]

Ransohoff RM, Perry VH. 2009 Microglial physiology: unique stimuli, specialized responses. Annu Rev Immunol 27:119–145. [PubMed: 19302036]

Saeed S, Quintin J, Kerstens HH, Rao NA, Aghajanirefah A, Matarese F, Cheng SC, Ratter J, Berentsen K, van der Ent MA, Sharifi N, Janssen-Megens EM, Ter Huurne M, Mandoli A, van Schaik T, Ng A, Burden F, Downes K, Frontini M, Kumar V, Giamarellos-Bourboulis EJ, Ouwehand WH, van der Meer JW, Joosten LA, Wijmenga C, Martens JH, Xavier RJ, Logie C, Netea MG, Stunnenberg HG. 2014 Epigenetic programming of monocyte-to-macrophage differentiation and trained innate immunity. Science 345:1251086. [PubMed: 25258085]

Salter MW, Beggs S. 2014 Sublime microglia: expanding roles for the guardians of the CNS. Cell 158:15–24. [PubMed: 24995975]

Sanagi T, Yuasa S, Nakamura Y, Suzuki E, Aoki M, Warita H, Itoyama Y, Uchino S, Kohsaka S, Ohsawa K. 2010 Appearance of phagocytic microglia adjacent to motoneurons in spinal cord tissue from a presymptomatic transgenic rat model of amyotrophic lateral sclerosis. J Neurosci Res 88:2736–2746. [PubMed: 20648658]

Satoh J, Tabunoki H, Ishida T, Yagishita S, Jinnai K, Futamura N, Kobayashi M, Toyoshima I, Yoshioka T, Enomoto K, Arai N, Arima K. 2011 Immunohistochemical characterization of microglia in Nasu-Hakola disease brains. Neuropathology 31:363–375. [PubMed: 21118401]

Sekiguchi A, Kanno H, Ozawa H, Yamaya S, Itoi E. 2012 Rapamycin promotes autophagy and reduces neural tissue damage and locomotor impairment after spinal cord injury in mice. J Neurotrauma 29:946–956. [PubMed: 21806471]

Tremblay ME, Lowery RL, Majewska AK. 2010 Microglial interactions with synapses are modulated by visual experience. PLoS Biol 8:e1000527. [PubMed: 21072242]

van der Knaap MS, Wassmer E, Wolf NI, Ferreira P, Topcu M, Wanders RJ, Waterham HR, Ferdinandusse S. 2012 MRI as diagnostic tool in early-onset peroxisomal disorders. Neurology 78:1304–1308. [PubMed: 22459681]

van Vliet EA, Forte G, Holtman L, den Burger JC, Sinjewel A, de Vries HE, Aronica E, Gorter JA. 2012 Inhibition of mammalian target of rapamycin reduces epileptogenesis and blood-brain barrier leakage but not microglia activation. Epilepsia 53:1254–1263. [PubMed: 22612226]

Verheijden S, Bottelbergs A, Krysko O, Krysko DV, Beckers L, De Munter S, Van Veldhoven PP, Wyns S, Kulik W, Nave KA, Ramer MS, Carmeliet P, Kassmann CM, Baes M. 2013 Peroxisomal multifunctional protein-2 deficiency causes neuroinflammation and degeneration of Purkinje cells independent of very long chain fatty acid accumulation. Neurobiol Dis 58:258–269. [PubMed: 23777740]

Yamasaki R, Lu H, Butovsky O, Ohno N, Rietsch AM, Cialic R, Wu PM, Doykan CE, Lin J, Cotleur AC, Kidd G, Zorlu MM, Sun N, Hu W, Liu L, Lee JC, Taylor SE, Uehlein L, Dixon D, Gu J, Floruta CM, Zhu M, Charo IF, Weiner HL, Ransohoff RM. 2014 Differential roles of microglia and monocytes in the inflamed central nervous system. J Exp Med 211:1533–1549. [PubMed: 25002752]

Zhan Y, Paolicelli RC, Sforazzini F, Weinhard L, Bolasco G, Pagani F, Vyssotski AL, Bifone A, Gozzi A, Ragozzino D, Gross CT. 2014 Deficient neuron-microglia signaling results in impaired functional brain connectivity and social behavior. Nat Neurosci 17:400–406. [PubMed: 24487234]

Main points

- Resident microglia in MFP2 deficient mice exhibit a proliferative and immunologically activated state but they lack signs of phagocytic and neurotoxic activity

- The chronically reactive microglia lose their typical homeostatic markers but upregulate pathways associated with growth and proliferation

- The molecular signature of microglia in *Mfp2*−/− brain strongly diverges from microglia in the neurodegenerative milieu of an ALS mouse model
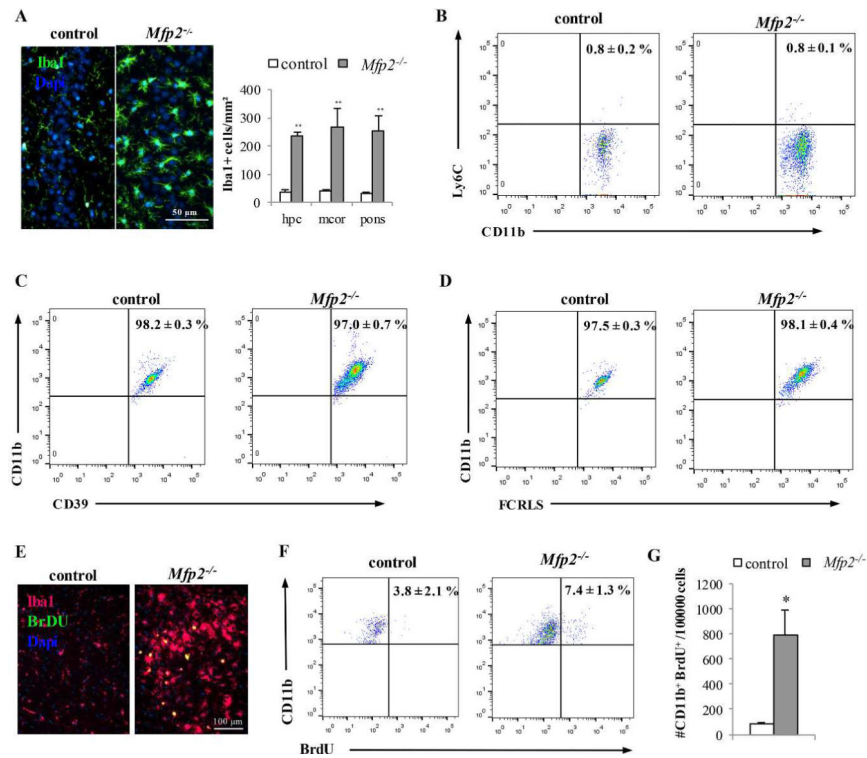
Figure 1. Increased numbers of myeloid cells in *Mfp2*^{−/−} brain do not derive from influx of peripheral monocytes but from proliferation of resident microglia

(A) Immunofluorescent staining for the microglia/macrophage marker Iba-1 reveals an increased number and altered shape of brain myeloid cells in the CA3 region of hippocampus in *Mfp2*$^{-/-}$ mice at 5 months compared to an age-matched control. Quantification of Iba-1$^+$ cells in different brain regions shows increased microglia cell numbers in hippocampus (hpc), motor cortex (mcor) and pons of *Mfp2*$^{-/-}$ mice (** $p <$ 0.01). Nuclei are stained blue with DAPI. (B) FACS analysis of Ly6C expression in CD11b-gated cells (n = 6 per group). Quantification shows that nearly all CD11b$^+$ cells in brain of control and *Mfp2*$^{-/-}$ mice are Ly6c negative. (C) Nearly all Cd11b myeloid cells from control and *Mfp2*$^{-/-}$ brain express the microglial specific surface marker CD39 (n = 6 per group). (D) Nearly all Cd11b$^+$ myeloid cells from control and *Mfp2*$^{-/-}$ brain express the microglial specific surface marker FCRLS (n = 4 per group). All FACS data are presented as mean ± SEM (n = 4– 6 per group) **$p < 0.01$. (E) BrdU incorporation (green) in Iba-1$^+$ cells (red) in *Mfp2*$^{-/-}$ but not in control brain using immunofluorescent staining. Nuclei are stained blue with DAPI. (F,G) BrDU incorporation in CD11b-gated cells is higher in *Mfp2*$^{-/-}$ compared to control mice (n = 3–4 per group, mean ± SEM) *$p < 0.05$.
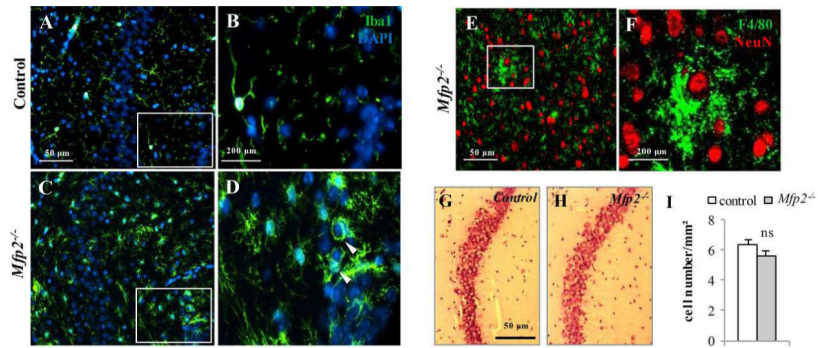
Figure 2. Abundant microglia-neuron contacts but no neuronal loss in *Mfp2*^{−/−} mice

(A-D) Activated microglia (Iba1$^+$, green) enwrap cell bodies (DAPI, blue) in the CA3 region of the hippocampus in *Mfp2*$^{-/-}$ mice (C,D) but not in control (A,B). B and D are magnifications of the highlighted area in A and C, respectively. Nuclei are stained blue with DAPI. (E) F4/80$^+$ cells contact NeuN neurons in the brainstem of *Mfp2*$^{-/-}$ mice. (F) Magnification of E. (G – I) H&E staining and quantification in the CA3 region of hippocampus reveals preservation of neurons in *Mfp2*$^{-/-}$ mice.
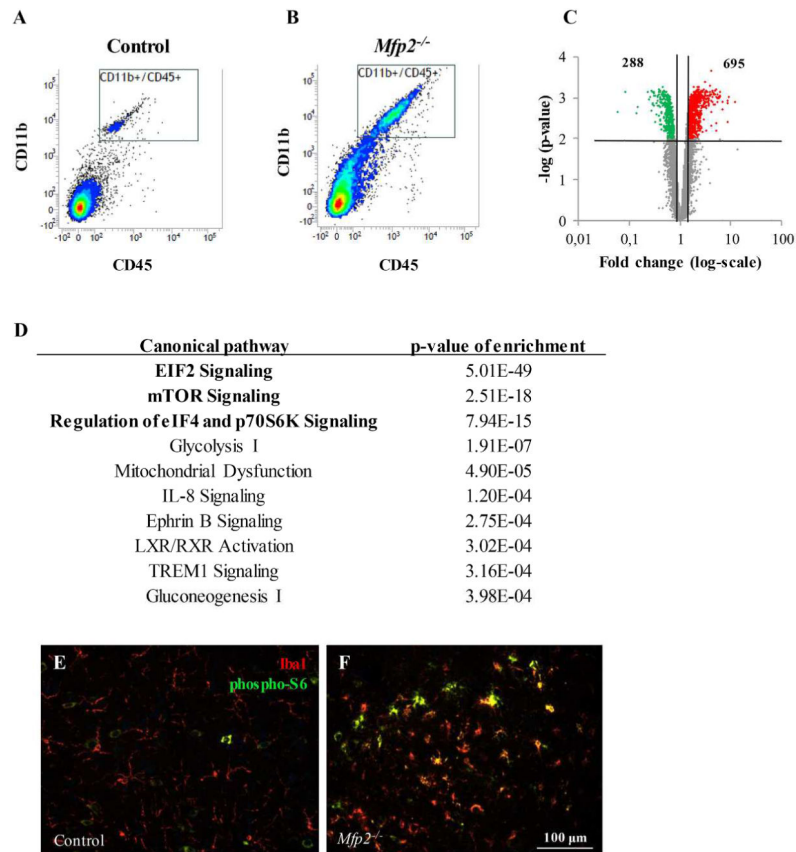
Figure 3. Transcriptomics analysis on acutely isolated microglia from control and *Mfp2*$^{-/-}$ mouse brain

(A,B) Cd11b/Cd45 FACS sorting of microglia isolated from control (A) and *Mfp2*$^{-/-}$ (B) mouse brain. (C) Volcano plot of differentially expressed genes of *Mfp2*$^{-/-}$ versus control microglia (cut-off: 0.75 ≥ fold change ≥ 1.5; p < 0.01). (D) The 10 most upregulated pathways after applying the canonical pathway enrichment tool of Ingenuity software on the microarray dataset of *Mfp2*$^{-/-}$ microglia (differentially expressed genes: 0.75 ≥ fold ≥ 1.5; p-value 0.01). (E,F) Increased IHC staining for phosphorylated ribosomal S6 (pS6, green), a downstream target of mTOR, in Iba1$^+$ microglia (red) in *Mfp2*$^{-/-}$ mice (F) as compared to control (E), shown for thalamus region.
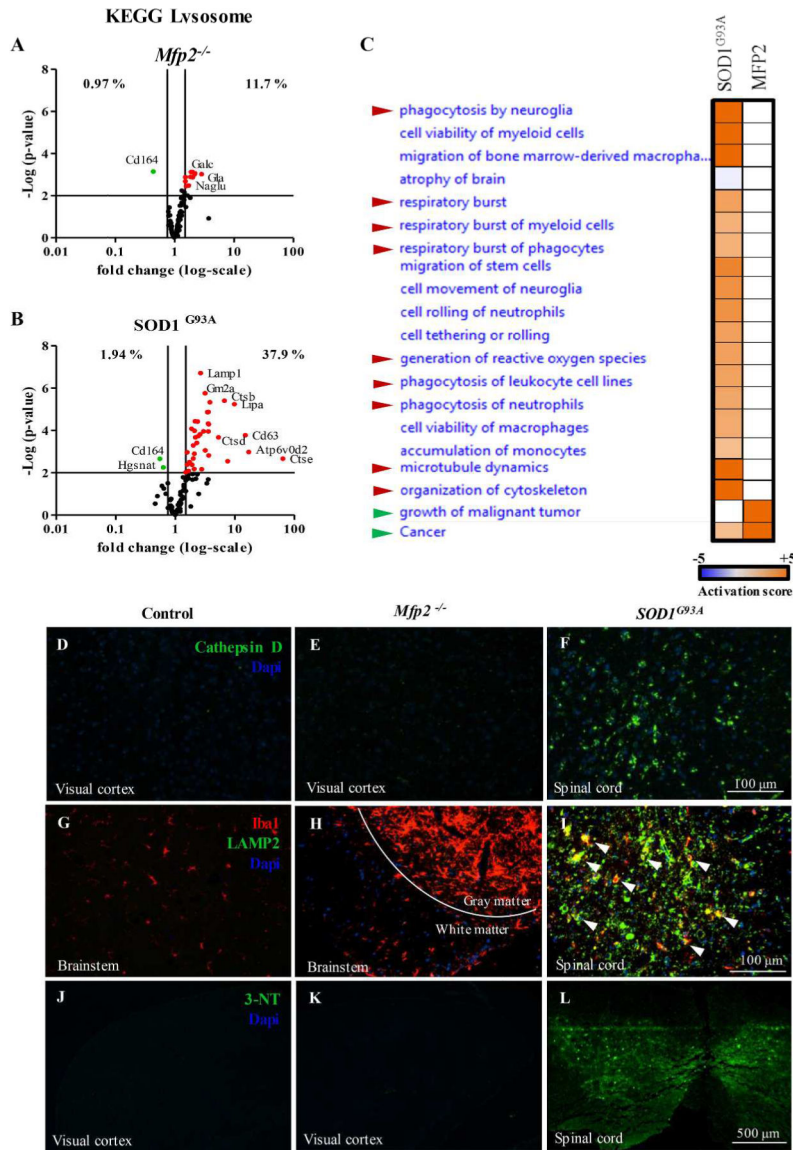
Figure 4. Differences in expression of lysosomal, phagocytic and nitrosative stress markers in *Mfp2−/−* versus *SOD1G93A* microglia

(A-B) After transcriptomics analyses of *Mfp2−/−* microglia (A) and *SOD1G93A* microglia (B) (data from GEO GSE43366) the expression of genes associated with the Lysosome (*mmu04142*) KEGG pathway were plotted. The percentage of genes of this pathway differentially expressed in both mouse models is shown. (C) Heatmap for enriched functions of *SOD1G93A* microglia as compared to *Mfp2−/−* microglia (Ingenuity analysis). Enrichment is depicted as activated (orange), not enriched (white) or deactivated (blue). Red arrows point to functions related to phagocytosis, green arrows to growth and proliferation. (D-F) Staining of the lysosomal marker Cathepsin D (green) in visual cortex of control (D) and *Mfp2−/−* mice (E) and in spinal cord of endstage SOD1G93A mice (F). (G-I) Co-staining of the microglial marker Iba1 (red) and the lysosomal marker LAMP2/MAC3 (green) in brainstem of control (G) and *Mfp2−/−* mice (H) and in spinal cord of endstage SOD1G93A mice (I). White arrowheads point to LAMP2+ microglia. (J-L) Staining for nitrosylated

proteins (green) in visual cortex of control (J) and *Mfp2*$^{-/-}$ mice (K) and in spinal cord of endstage SOD1^{G93A} mice (L). Nuclei are stained blue with DAPI.
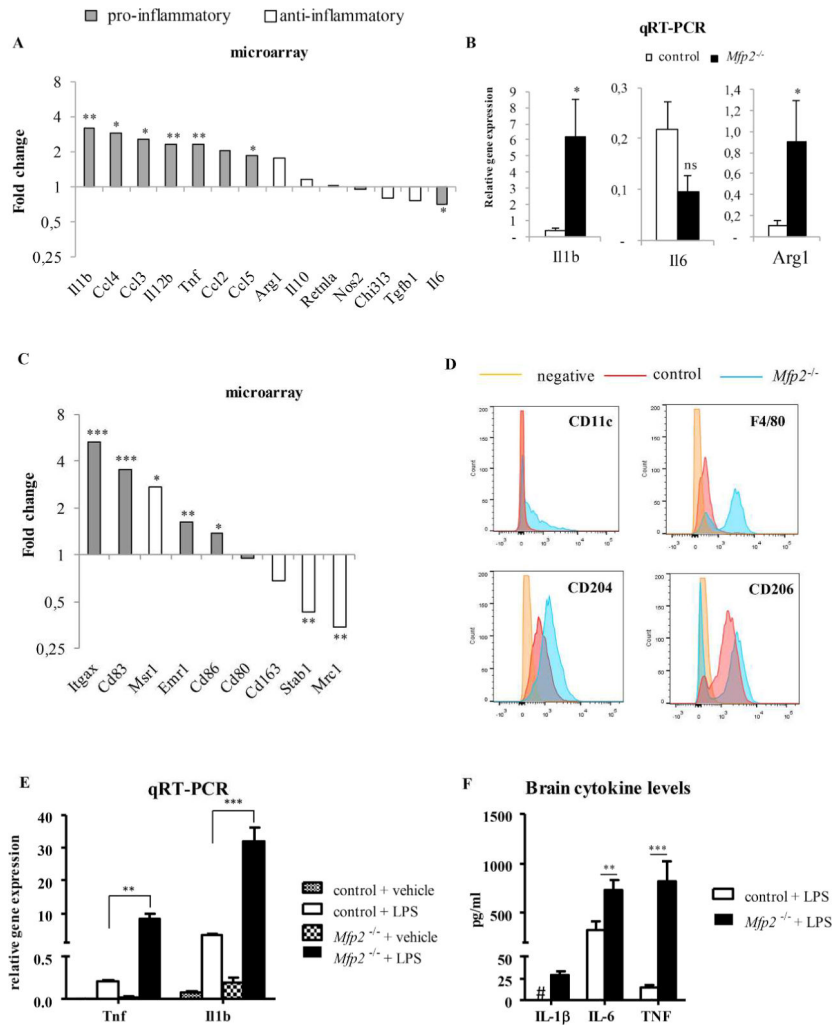
Figure 5. The immunological profile of *Mfp2*^{−/−} microglia is not polarized to a pro- or antiinflammatory state

(A) Relative transcript levels of pro-inflammatory (dark gray bars) and anti-inflammatory (white bars) activation markers as determined by microarray analysis in *Mfp2*^{−/−} microglia compared to wild type (n=4). (B) qRT-PCR analyses of the pro-inflammatory markers IL1β and IL6 and the anti-inflammatory marker Arg-1 confirm micro-array data and indicate that microglia are not unequivocally polarized. mRNA expression levels were normalized to β-actin. Data are presented as mean ± SEM (n = 3–4). * p < 0.05; ** p < 0.01. (C) Surface markers expression associated with classical (gray) and alternative (white) macrophage activation as determined by microarray analysis. (D) FACS analysis of CD11b⁺ microglia shows increased expression of CD11c and F4/80 surface markers associated with classical activation. There is also increased expression of the anti-inflammatory marker CD204^{pos} (Msr1) as well as an increase in the proportion of microglia that are CD206^{neg} (Mrc1) (representative experiment out of two). (E-F) *Mfp2*^{−/−} and control mice (n=3–5) were challenged with intraperitoneal LPS and brainstem tissue was analyzed after 4 hrs. Transcripts (E) and cytokine levels (F) of *Il1b, Il6* and *Tnf* were more elevated in *Mfp2*^{−/−} as compared to control mice. # = not detectable, * p<0.05, ** p < 0.01, ***p<0.001.
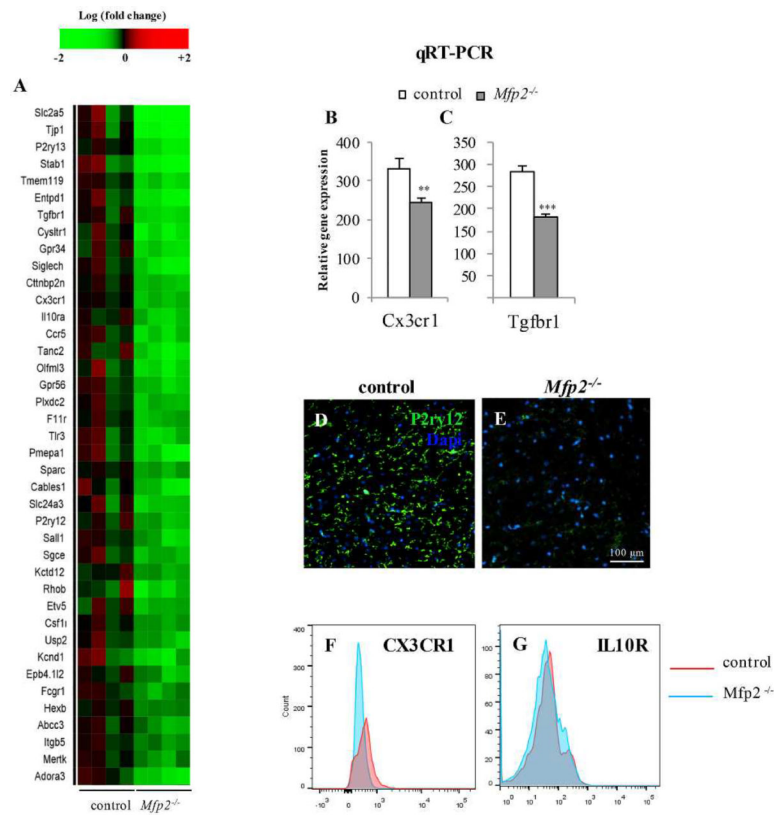
Figure 6. Repression of homeostatic gene signature in *Mfp2*−/− microglia

(A) Heatmap showing expression values of signature genes of microglia (according to Butovsky et al, 2013) in control versus *Mfp2*−/− microglia. In *Mfp2*−/− microglia, 40 out of 86 genes are significantly downregulated (47%). Expression values are expressed as robust multi-array analysis (RMA). (B,C) qRT-PCR confirms the downregulation of the microglia-enriched genes *Cx3cr1* (A) and *Tgfbr1* (B) in *Mfp2*−/− microglia. Expression levels were normalized to β-actin. Data are presented as mean ± SEM (n = 3–4, ** p < 0.01; *** p < 0.001). (D,E) Immunohistochemical staining confirms downregulation of the purinergic receptor P2RY12 on microglia of *Mfp2*−/− as compared to wild type mice. (F,G) FACS analysis of CD11b+ microglia shows reduced expression of CX3CR1 and to a lesser extent of IL10R in *Mfp2*−/− microglia (1 experiment out of 2 with similar data).